Opto-Electronics Review 28 (2020) 191–196

PAN POLISH ACADEMY OF SCIENCES

Opto-Electronics Review

journal homepage: http://journals.pan.pl/opelre

Electronic, optical and non-linear optical properties of an *N*-cyclohexylacrylamide molecule: a potential optoelectronic agent

E. Tanış[a*], N. Çankaya[b]

[a] Department of Electrical Electronics Engineering, Kırşehir Ahi Evran University, 40100 Kırsehir, Turkey
[b] Department of Chemistry, Uşak University, 64300, Uşak, Turkey.

Article info

Article history:
Received 26 Mar. 2020
Received in revised form 29 Jun. 2020
Accepted 03 Sep. 2020

Keywords:
N-cyclohexylacrylamide, electronic properties, optical properties, non-linear optical properties, DFT

Abstract

In this article, synthesis, electronic and optical properties of an *N*-cyclohexylacrylamide (NCA) molecule are described based on different solvent environments and supported by theoretical calculations. Theoretical calculations have been carried out using a density function theory (DFT). Temperature dependence of the sample electrical resistance has been obtained by a four-point probe technique. Experimental and semi-theoretical parameters such as optical density, transmittance, optical band gap, refractive index of the NCA for different solvents were obtained. Both optical values and electrical resistance values have shown that NCA is a semiconductor material. The values of HOMO and LUMO energy levels of the headline molecule indicate that it can be used as the electron transfer material in OLEDs. All results obtained confirm that the NCA is a candidate molecule for OLED and optoelectronic applications.

1. Introduction

Organic semiconductors have attracted great attention in the past few years due to their low cost and large-scale organic device potential. These devices include electronics, optoelectronics, organic photovoltaic applications [1-4], organic light emitting diodes [5,6], sensors [7-10], photodetectors [11], transistors [12], radio frequency identification tags [13], and large area integrated circuits [14]. They are also promising for solid-state lighting that emits efficient white light emitting devices (WOLEDs) [15]. In this context, we investigated *N*-cyclohexylacrylamide (NCA), an acrylamide-based semiconductor.

There are many studies about acrylamide-added gels to be used as a glucose sensing material due to their structural and optical properties [16-18]. In addition, polymers with acrylamide additive have application areas in soft electronic devices and sensors with their unique properties [19].

It is known that structural and optical properties of an organic molecule strongly influenced the solvent medias [20-22]. Solvent environments, which cause important changes in the properties of materials, significantly affect the designed devices performance [23].

In this study, electronic, optical properties of the NCA molecule, an organic semiconductor, and its suitability for optoelectronic applications in various solvent environments were investigated. Both experimental techniques and theoretical methods were used. Firstly, theoretically the most stable structure of the NCA was determined using a density function theory (DFT) method. Later, ultraviolet-visible (UV-Vis) spectra, frontier molecular orbitals (HOMO and LUMO), energy difference between these orbitals (E_g) for different solvents: acetonitrile (ACN), dimethyl sulfoxide (DMSO) and dimethylformamide (DMF) were calculated using a TD-DFT/B3LYP method. Calculated E_g values were compared with experimental ones for different solvents. Non-linear optical

* Corresponding author at: eminetanis@ahievran.edu.tr

https://doi.org/10.24425/opelre.2020.135257

properties and spectra of a total density of state (TDOS or DOS), and a partial density of state (PDOS) were calculated and discussed in detail. The refractive index (n) was calculated using semi-experimental methods on experimental E_g data. It was determined that the solvent effect on the $(\alpha h\vartheta)^2$ curves connected to the photon energy (E). Electrical resistance change of NCA with temperature was measured using the four-point probe technique [24]. Experimental results have been compared with theoretical and semi-theoretical values.

2. Experimental details

2.1 Materials

NCA was previously synthesized and characterized by our team and all chemicals required for its synthesis were used in analytical purity, including acrylic chloride, cyclohexyl amine, triethyl amine, and solvents [25,26]. In Fig. 1, the NCA synthesis scheme is given.

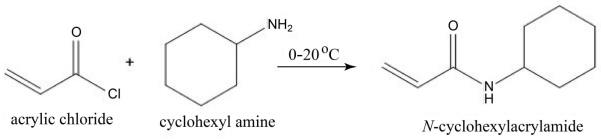

Fig. 1. Synthesis scheme of the NCA.

2.2 Experimental details

Optical measurements of the solutions of the NCA in ACN, DMSO and DMF solvents were recorded with a solution technique using a UV-1800 Spectrophotometer at room temperature. Electrical resistance change of the sample depending on temperature was obtained with the four-point probe technique [24]. Details on the experimental procedure are available in the above reference.

3. Computational details

All calculations were made in the Gaussian 09 program [27] using DFT calculations based on a B3LYP change correlation which is functionally based on6-311++G(d,p) [28]. The NCA molecule optimized with DFT/B3LYP/6-311++G(d,p) is presented in Fig. 2. Electronic, non-linear optical properties and E_g values were calculated and compared with the observed ones of the studied molecule. GaussSum 2.2 program [29] was used to analyze the spectra of DOS and PDOS molecular orbitals.

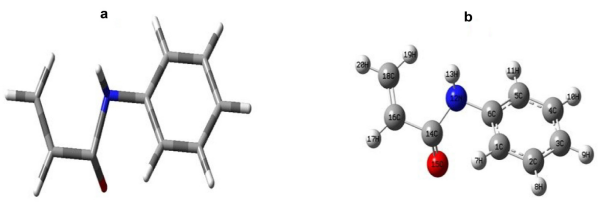

Fig. 2. Structures of the NCA molecule: a) 2D, b) 3D.

4. Results and discussion

4.1 Experimental results

Absorbance or optical density spectra of the NCA molecule in ACN, DMSO and DMF solvents were taken and shown in Fig. 3. The absorption spectrum of NCA in ACN and DMSO exhibited a maximum peak at 285 nm, while for DMF solvent - at 268 nm. Furthermore, the NCA molecule showed only a single peak for each of three solvents in the respective wavelength as seen in Fig. 3. Also, as can be seen, the NCA absorbance curve remains constant at the lowest values at wavelengths greater than about 300 nm. These results show that the absorption spectra of the NCA molecule have a middle ultraviolet (MUV) region of the absorption spectrum.

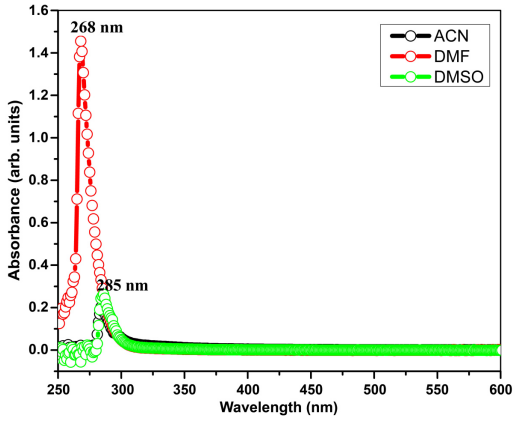

Fig. 3. Absorbance spectra of the NCA for different solvents.

Transmittance (T) plays an important role in optical properties. Figure 4 indicates the transmittance spectra of the NCA molecule in ACN, DMSO and DMF solvents. As seen in Fig. 4, the transmittance spectra of the NCA exhibit a peak characteristic in the MUV region, while they remain constant at the maximum values in the near visible (NUV) region. In the MUV region, the NCA absorption and transmittance values increase as the solvent dielectric constant increases. The solvent with a larger dielectric constant produces greater stabilization energy for polar species [30]. The stabilizing effect of DMSO ($\varepsilon = 46.7$) is greater than the DMF ($\varepsilon = 36.7$) and NCA ($\varepsilon = 37.5$). As a result, absorbance and transmittance values in DMSO were higher than in ACN and DMF.

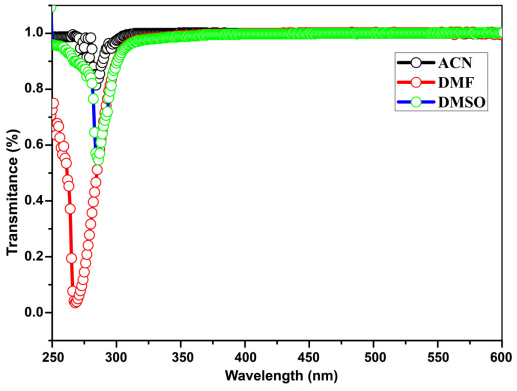

Fig. 4. The transmittance spectra of the NCA for different solvents.

Optical band gap (E_g) is a fundamental optical parameter and can be obtained from Tauc model [30]. Firstly, we determined a type of optical transitions [31], where the allowed direct band gap (E_{gd}) is suitable for the NCA molecule. Figure 5 shows the $(\alpha h\vartheta)^2$ curves *vs.* the photon energy (E) of the NCA in ACN, DMF and DMSO solvents, respectively. E_{gd} values of NCA in ACN, DMSO and DMF solvents were obtained by extrapolating the linear plot to $(\alpha h\vartheta)^2 = 0$ and were given in Table 1.

Table 1.
The optical band gap (E_g) parameters of the NCA molecule for different solvents.

Solvents	E_g (eV)
ACN	4.2
DMF	4.2
DMSO	4.15

The electrical resistance (ρ) change of NCA with temperature was measured using the four-point probe technique [24]. The sample electrical resistance was determined using the following equation [32]:

$$\rho = 2\pi s \cdot V/I\,, \qquad (1)$$

where V is the potential drop, I is the current and s is the distance between probe tips. Data on the temperature dependent changes of the resistivity of NCA are given in Table 2. The resistivity data in Table 2 indicate that results change in between 7.10×10^5 and 5.19×10^7 Ω·cm at ambient temperature. Electrical resistances of the semiconductors at room temperature range from 10^{-2} to 10^9 Ω·cm [32]. Table 2 shows that the resistivity of NCA falls in this range. Both the optical band gap (E_g) values in Table 1 and the electrical resistivity (ρ) values in Table 2 show that NCA has semiconductor properties.

Table 2.
The temperature dependent change of the resistivity of NCA.

Temperature (K)	Electrical resistivity (Ω·cm)
299	7.10×10^5
313	4.47×10^6
326	6.23×10^6
340	8.74×10^6
351	1.08×10^7
362	6.64×10^6
374	4.83×10^6
391	4.43×10^6
407	1.10×10^7
419	5.19×10^7

Refractive indices of the NCA in DMSO, ACN and DMF solvents and for many semi-theoretical relations such as Herve-Vandamme, Kumar-Singh, Moss, Ravindra, and Reddy [33] were obtained and given in Table 3.

Table 3.
The experimental (1) and semi-theoretical refractive indices obtained from Moss (2), Ravindra (3), Herve-Vandamme (4), Reddy (5), Kumar-Singh (6) relations and their average values (7) of the NCA molecule for different solvents.

	Refractive indices (n)						
Solvents	**1**	**2**	**3**	**4**	**5**	**6**	**7**
ACN	2.34	2.18	1.48	2.03	2.51	2.11	2.06
DMF	2.61	2.18	1.48	2.03	2.51	2.11	2.06
DMSO	2.40	2.19	1.51	2.04	2.52	2.12	2.07

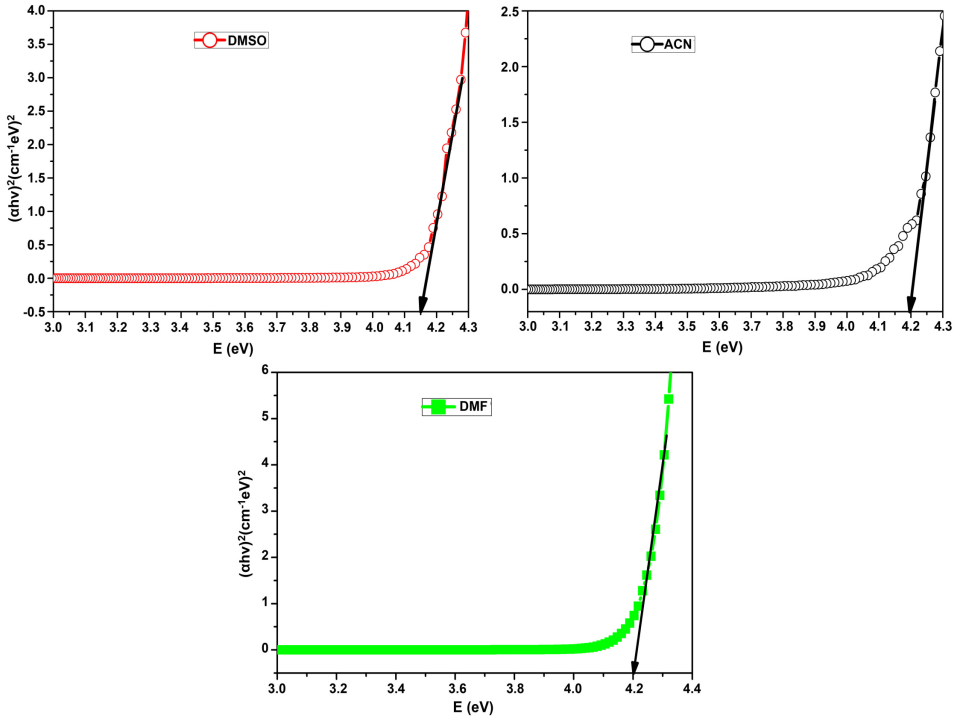

Fig. 5. The $(\alpha h\vartheta)^2$ curves *vs.* the photon energy (E) of the NCA for different solvents.

Using these relations, the experimental E_g values shown in Fig. 5 were used to obtain the experimental results in Table 3, and the theoretical E_g values shown in Fig. 6 were used to obtain the semi-theoretical results. As seen in Table 3, the refractive index values of NCA are the same in DMF and ACN solvents and different in DMSO solvent. The average refractive index values of NCA appear to vary between 2.06 and 2.07. These values can be considered as suitable for semiconductor and OLED materials. And the lowest refractive index is observed for Ravindra relation, while the highest refractive index is observed for Reddy relation. In addition, the experimental refractive index values are larger than semi-theoretical refractive indices.

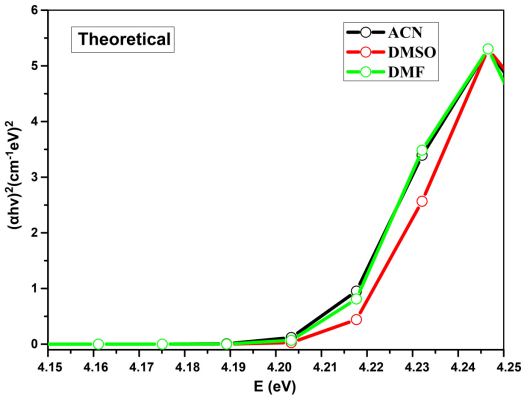

Fig. 6. The $(\alpha h\vartheta)^2$ curves *vs*. E for NCA computed from B3LYP/6-311++G (d,p) level of theory.

4.2 Theoretical results

4.2.1 Frontier molecular orbitals analysis

E_g values were calculated as 4.21 and 4.22 eV for ACN, DMF and DMSO solvents, respectively. Experimental E_g values were found as 4.20 and 4.15 eV in ACN, DMF and DMSO solvents, respectively. When the calculated and measured E_g values are compared, it can be seen that they are quite compatible with each other (see Figs. 5 and 6).

The frontier molecular orbitals (FMOs) energy was obtained by B3LYP/6-311++G(d,p) method in gas phase. HOMO-LUMO shapes for the molecule are given in Fig. 7. The high value of HOMO indicates that electrons have a high interest in a suitable receptor molecule.

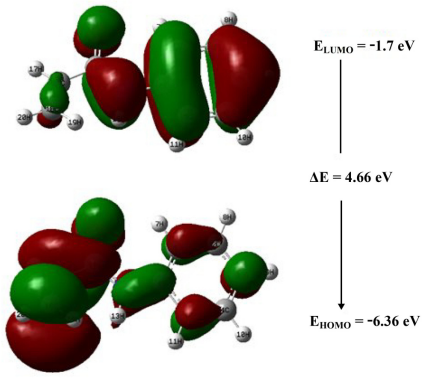

Fig. 7. The frontier molecular orbitals of the NCA for gas phase.

Similarly, the low value of LUMO indicates that there is a high interest in accepting electrons [34,35]. HOMO orbitals or valence band were mostly spread over the acrylamide group, while LUMO orbitals or conductivity band were mostly spread over the cyclohexyl group.

The energy gap, which is the energy difference between HOMO and LUMO orbital, is an important parameter in determining conductivity. As shown in Fig. 7, this value for NCA is of 4.66 eV in gas phase. In this context, the NCA molecule is a semiconductor material with the energy range of 4.66 eV.

4.3 NLO (non-linear optical) analysis

NLO materials have extensive application areas such as storage, optical switching, communication, optical sensors, displays, and signal processing [36-38]. Theoretical calculations provide sufficient and reliable results in the investigation of new nonlinear materials. In this study, the electrical dipole moment (μ), hyper-polarizability (β) and polarizability (α) values from NLO properties were investigated using the B3LYP/6-311++G(d,p) basis set to understand the optical and electrical response of NCA. This values were provided *via* the Gaussian output file and their atomic units (a.u.) were converted to electronic units (esu) (1 a.u. = 0.1482×10^{-24} esu for α; 1 a.u. = 8.6393×10^{-33} esu for β). The values of mean polarizability (α), anisotropy of polarizability ($\Delta\alpha$), mean molecular hyperpolarizability (β), and total dipole moments were calculated using the equations below:

$$\alpha_{tot} = \frac{1}{3}(\alpha_{xx} + \alpha_{yy} + \alpha_{zz}) \quad (2)$$

$$\Delta\alpha = \frac{1}{\sqrt{2}}\left[(\alpha_{xx} - \alpha_{yy})^2 + (\alpha_{yy} - \alpha_{zz})^2 + (\alpha_{zz} - \alpha_{xx})^2 + 6\alpha_{xz}^2 + 6\alpha_{xy}^2 + 6\alpha_{yz}^2\right]^{\frac{1}{2}} \quad (3)$$

$$\langle\beta\rangle = \left[(\beta_{xxx} + \beta_{xyy} + \beta_{xzz})^2 + (\beta_{yyy} + \beta_{yzz} + \beta_{yxx})^2 + (\beta_{zzz} + \beta_{zxx} + \beta_{zyy})^2\right]^{\frac{1}{2}} \quad (4)$$

$$\mu_{tot} = (\mu_x^2 + \mu_y^2 + \mu_z^2)^{\frac{1}{2}}. \quad (5)$$

The calculated values are presented in Table 4. As organic light emitting diodes are used, optically active materials NLO properties are important to interpret their optoelectronic responses.

For a molecule to behave like a good NLO material, the first hyperpolarizability, dipole moment and polarity must be large. The magnitude of these values is generally interpreted relative to the values of urea. In this study, the values of β_{tot} and $\Delta\alpha$ are calculated as $1850.816685\text{x}10^{-33}$esu and $45.1074\text{x}10^{-24}$ esu, respectively. These values for urea are: $\beta_{tot} = 194.7\text{x}10^{-33}$ esu and $\Delta\alpha = 3.8312\text{x}10^{-24}$ esu. It can be seen that the first order hyper-polarizability value of the NCA is approximately 10 times higher than that of urea, and, similarly, the mean polarizability is about 12 times larger. These results show that the NCA can be used as a high NLO material for future applications.

Table 4.
The dipole moments μ (D), the polarizability α (a.u.), the average polarizability α_o ($\times 10^{-24}$ esu), the anisotropy of the polarizability $\Delta\alpha$ ($\times 10^{-24}$ esu), and the first hyperpolarizability β ($\times 10^{-33}$ esu) of NCA.

μ_x	-0.4241	β_{xxx}	4.5418
μ_y	-3.629500	β_{xxy}	892.9641
μ_z	-0.013500	β_{xyy}	-5.6564
μ_0	3.654219	β_{yyy}	991.9187
α_{xx}	25.2057	β_{xxz}	-2.1735
α_{xy}	0.26668	β_{xyz}	-2313.4629
α_{yy}	16.1501	β_{yyz}	0.0410
α_{xz}	1.2850	β_{xzz}	4.2981
α_{yz}	3.6375	β_{yzz}	-14.0939
α_{zz}	12.4811	β_{zzz}	0.7151
α_{total}	11799.3876	β_x	2.9842475
$\Delta\alpha$	45.1074	β_y	1250.7888
		β_z	-2.145689
		β	1850.816685

4.3.1 Density of states (DOS and PDOS)

The energies of molecular orbitals located close to each other in the boundary regions of the molecule can be semi-degenerate. Therefore, the boundary molecular orbitals of a molecule may not be sufficient to describe only HOMO and LUMO. [39]. In this frame of reference, DOS and PDOS density of states [40-42] were calculated and formed *via* GaussSum2.2 program by convoluting the molecular orbital information with Gaussian curves of unit height with full width at half maximum (FWHM) of 0.3 eV. DOS and PDOS graphs are presented in Figs. 8 and 9. Figure 9 shows the orbital energy values of interactions between some selected groups. According to this graph, the cyclohexyl group made the biggest contribution to all orbitals.

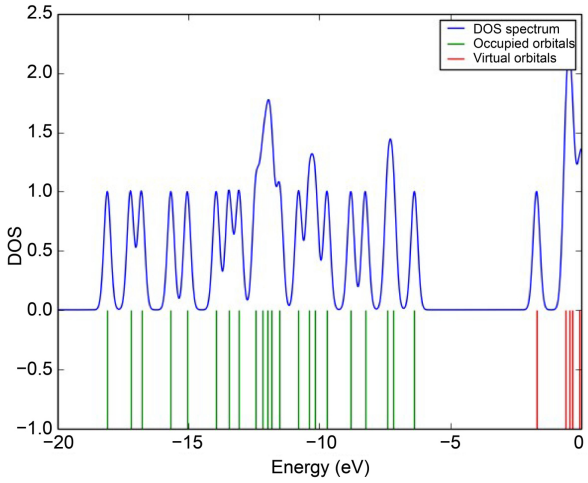

Fig. 8. The total electronic density of states (TDOS) diagram of the NCA.

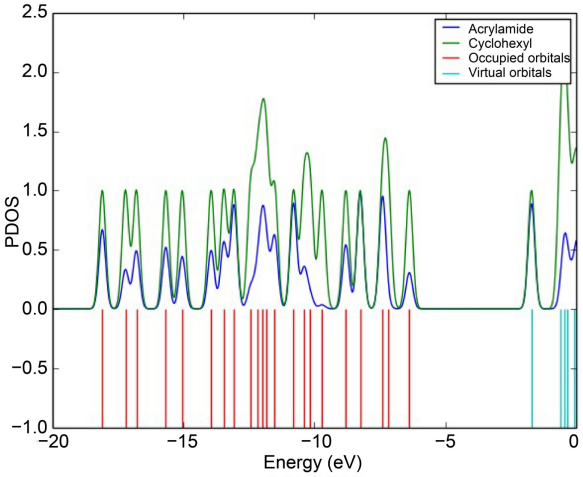

Fig. 9. The partial electronic density of states (PDOS) diagram of the NCA.

5. Conclusions

In this study, firstly, the *N*-cyclohexylacrylamide was synthesized according to literature. Electronic, optical and non-linear optical properties of the NCA molecule were investigated by both experimental techniques and theoretical methods. Both experimentally and theoretically, the same results were obtained for ACN and DMF solvents, while different results were obtained for DMSO solvent. The optical band range of NCA obtained both experimentally and theoretically showed that it is a material suitable for OLED technology. The electrical resistivity of NCA is compatible with that of semiconductors. The variation of refractive index with the solvent effect was also investigated using semi-experimental methods. It was determined that the refractive index of NCA for all solvents was in semiconductor value range. From the PDOS results, it is seen that the cyclohexyl group in the molecule contributes most to the electronic band structure of NCA. Furthermore, header molecule hyperpolarizability, dipole moment and polarizability were obtained. The first-order hyperpolarizability of NCA was calculated 10 times higher than that of urea ($\beta = 0.37\text{x}10^{-30}$ esu) and the mean polarizability was calculated 12 times greater than that of urea ($\Delta\alpha = 3.83\text{x}10^{-24}$). The results showed that the NCA could be a good NLO material. Furthermore, DMSO solvent can be preferred for the OLEDs device with a lower optical band gap.

References

[1] Sutton, C., Sears, J. S., Coropceanu, V. & Breas, J. L. Understanding the Density Functional Dependence of DFT-Calculated Electronic Couplings in Organic Semiconductors. *J. Phys. Chem. Lett*. **4,** 919−924 (2013). https://doi.org/10.1021/jz3021292.

[2] Bouchouit, K. *et al*. Investigation of crystal structure and nonlinear optical properties of 2-methoxyanilinium nitrate. *Opt. Commun*. **278,** 180–186 (2007). https://doi.org/10.1016/j.optcom.2007.05.068.

[3] Bouchouit, K. *et al*. Experimental and theoretical studies of NLO properties of organic–inorganic materials base on p-nitroaniline. *Chem. Phys. Lett.* **455**, 270–274 (2008). https://doi.org/10.1016/j.cplett.2008.02.101.

[4] Bouchouit, K., Bougharraf, H., Derkowska-Zielinska, B., Benali-Cherif, N. & Sahraoui, B. Reversible phase transition in semi-

organic compound p-Nitroanilinium sulfate detected using second harmonic generation as a tool. *Opt. Mater*. **48**, 215-221 (2015). https://doi.org/10.1016/j.optmat.2015.07.035

[5] Xiao-Hong, L., Hong-Ling, C., Rui-Zhou, Z. & Xian-Zhou, Z. Theoretical investigation on the non-linear optical properties, vibrational spectroscopy and frontier molecular orbital of (E)-2-cyano-3-(3-hydroxyphenyl)acrylamide molecule. *Spectroc. Acta Pt. A-Molec. Biomolec. Spectr*. **137,** 321–327 (2015). https://doi.org/10.1016/j.saa.2014.08.036.

[6] Ameen, M.Y., Abhijith, T., Susmita, D., Ray, S.K. & Reddy, V.S. Linearly polarized emission from PTCDI-C8 one-dimensional microstructures. *Org. Electron.* **14,** 554–559 (2013). https://doi.org/10.1016/j.orgel.2012.12.012.

[7] Aziz, F. *et al*. Influence of humidity conditions on the capacitive and resistive response of an Al/VOPc/Pt co-planar humidity sensor. *Meas. Sci. Technol.* **23,** 014001–014009 (2012). https://doi.org/10.1088/0957-0233/23/1/014001.

[8] Murugavelu, M., Imran, P.K.M., Sankaran, K.R. & Nagarajan, S. Self-assembly and photophysical properties of a minuscule tailed perylene bisimide. *Mater. Sci. Semicon. Proc.* **16**, 461–466 (2013). https://doi.org/10.1016/j.mssp.2012.08.001.

[9] Harsaanyi G. Polymer films in sensor applications: a review of present uses and future possibilities. *Sens. Rev.* **20**, 98–105 (2000). https://doi.org/10.1108/02602280010319169.

[10] Che, Y. *et al*. Ultrathin n-Type Organic Nanoribbons with High Photoconductivity and Application in Optoelectronic Vapor Sensing of Explosives. *J. Am. Chem. Soc*. **132**, 5743–5750 (2010). https://doi.org/10.1021/ja909797q.

[11] Guan, M. *et al*. Organic light-emitting diodes with integrated inorganic photo detector for near-infrared optical up-conversion, *Org. Elec.* **12,** 2090–2094 (2011). https://doi.org/10.1016/j.orgel.2011.09.003.

[12] Tseng, H.R. *et al*. High-Mobility Field-Effect Transistors Fabricated with Macroscopic Aligned Semiconducting Polymers. *Adv. Mater*. **26,** 2993–2998 (2014). https://doi.org/10.1002/adma.201305084.

[13] Hadziioannou, G. & Malliaras, G. *Semiconducting Polymers*, 768 (Wiley-VCH: Weinheim, Germany, 2007).

[14] Liu, Z., Kobayashi, M., Paul, B.C., Bao, Z. & Nishi, Y. Contact engineering for organic semiconductor devices via Fermi level depinning at the metal-organic interface. *Phys. Rev. B* **82**, 035311–035317(2010) https://doi.org/10.1103/PhysRevB.82.035311.

[15] Sun, Y.R. *et al*. Management of singlet and triplet excitons for efficient white organic light-emitting devices. *Nature* **440**, 908-912 (2006). https://doi.org/10.1038/nature04645.

[16] Domschke, A., March, W.F., Kabilan, S. & Lowe, C. Initial clinical testing of a holographic noninvasive contact lens glucose sensor. *Diabetes Technol. Ther*. **8,** 89–93 (2006). https://doi.org/10.1089/dia.2006.8.89.

[17] Alexeev, V.L., Das, S., Finegold, D.N. & Asher, S.A. Photonic crystal glucose-sensing material for noninvasive monitoring of glucose in tear fluid. *Clin. Chem.* **50**, 2353–2360 (2004). https://doi.org/10.1373/clinchem.2004.039701.

[18] Hu,Y., Jiang, X., Zhang, L., Fan, J. & Wu, W. Construction of near-infrared photonic crystal glucose-sensing materials for ratiometric sensing of glucose in tears. *Biosens. Bioelectron*. **48**, 94–99 (2013). https://doi.org/10.1016/j.bios.2013.03.082.

[19] Dzhardimalieva, G.I., Yadav, B.C., Singh, S. & Uflyand, I.E. Self-healing and shape memory metallopolymers: state-of-the-art and future Perspectives. *Dalton Trans.* **49**, 3042–3087 (2020). https://doi.org/10.1039/C9DT04360H.

[20] Van Duren, J. K. J. *et al*. Relating the morphology of poly(p - phenylene vinylene) / methanofullerene blends to solar - cell performance. *Adv. Func. Mater*. **14**, 425–434 (2004). https://doi.org/10.1002/adfm.200305049.

[21] Hoppe, H. *et al*. Sariciftci, N. S., Nanoscale morphology of conjugated polymer/fullerene - based bulk - heterojunction solar cells. *Adv. Funct. Mater*. **14**, 1005–1011 (2004). https://doi.org/10.1002/adfm.200305026.

[22] Jeon, B.C. *et al*. Effect of solvent on dye-adsorption process and photovoltaic properties of dendritic organic dye on TiO2 electrode of dye-sensitized solar cells. *Synth. Met.* **188**, 130-135 (2014). https://doi.org/10.1016/j.synthmet.2013.12.006.

[23] Liu, Y. *et al*. Theoretical investigation of solvent effects on tautomeric equilibrium of 2-diazo-4,6-dinitrophenol. *Int. J. Quant. Chem.* **111**, 1115–1126 (2011). https://doi.org/10.1002/qua.22468.

[24] Erat, S., Metin, H. & Ari, M. Influence of the annealing in nitrogen atmosphere on the XRD, EDX, SEM and electrical properties of chemical bath deposited CdSe thin films. *Mater. Chem. Phys.* **111**, 114–120 (2008). https://doi.org/10.1016/j.matchemphys.2008.03.021.

[25] Çankaya, N. Synthesis of graft copolymers onto starch and its semiconducting properties. *Results Phys.* **6**, 538–542 (2016). https://doi.org/10.1016/j.rinp.2016.08.010.

[26] Daşbaşı, T., Saçmacı, Ş., Çankaya, N. & Soykan, C. Synthesis, characterization and application of a new chelating resin for solid phase extraction, preconcentration and determination of trace metal ions in some dairy samples by flame atomic absorption spectrometry. *Food Chem.* **211**, 68–73 (2016). https://doi.org/10.1016/j.foodchem.2016.05.037.

[27] Frisch, M. J. *et al*. Gaussian 09, Revision A.2, Gaussian, Inc., Wallingford, CT, 2009.

[28] Becke, A. D. Density-functional exchange-energy approximation with correct asymptotic behavior. *Phys. Rev. A* **38**, 3098 (1988). http://dx.doi.org/10.1063/1.464304.

[29] O'Boyle, N. M., Tenderholt, A. L. & Langner, K. M. cclib: A library for package-independent computational chemistry algorithms. *J. Comp. Chem.*, **29,** 839–845 (2008), https://doi.org/10.1002/jcc.20823.

[30] Fan, J. C., Shang, Z .C., Liang, J., Liu, X. H. & Jin, H. Systematic theoretical investigations on the tautomers of thymine in gas phase and solution. *J. Mol. Struct–Theochem*. **939,** 106–111 (2010). https://doi.org/10.1016/j.theochem.2009.09.047.

[31] Tokuhisa, H., Era, M., Tsutsui, T. & Saito, S. Electron drift mobility of oxadiazole derivatives doped in polycarbonate. *Appl. Phys. Lett.* **66**, 3433–3435 (1995). https://doi.org/10.1063/1.113378.

[32] Sat, F. Conductivity measurements in semiconductors, Mersin University Graduate School of Natural and Applied Sciences, (2010).

[33] Tripathy, S.K. Refractive indices of semiconductors from energy gaps. *Opt. Mater*. **46** 240–246 (2015). https://doi.org/10.1016/j.optmat.2015.04.026.

[34] Tanış, E., Çankaya, N. & Yalçın, S. Synthesis, characterization, computation of global reactivity descriptors and antiproliferative activity of N-(4-nitrophenyl)acrylamide, *Russ. J. Phys. Chem. B* **13**, 49–61 (2019). https://doi.org/10.1134/S1990793119010147.

[35] Helal, M.H. *et al*., Synthesis, biological evaluation and molecular modeling of novel series of pyridine derivatives as anticancer, anti-inflammatory and analgesic agents. *Spectroc. Acta Pt. A* **135**, 764–773 (2015). https://doi.org/10.1016/j.saa.2014.06.145.

[36] Muthu, S.J. & Maheswari, U. Quantum mechanical study and spectroscopic (FT-IR, FT-Raman, 13C, 1H, UV) study, first order hyperpolarizability, NBO analysis, HOMO and LUMO analysis of 4-[(4-aminobenzene) sulfonyl] aniline by ab initio HF and density functional method. *Spectroc. Acta Pt. A* **92**, 154–163 (2012). https://doi.org/10.1016/j.saa.2012.02.056.

[37] Govindarasu, K. & Kavitha, E. Vibrational spectra, molecular structure, NBO, UV, NMR, first order hyperpolarizability, analysis of 4-Methoxy-4′-Nitrobiphenyl by density functional theory. *Spectroc. Acta Pt. A* **122**, 130–141 (2014). https://doi.org/10.1016/j.saa.2013.10.122.

[38] Govindarasu, K., Kavitha, E. & Sundaraganesan, N. Synthesis, structural, spectral (FTIR, FT-Raman, UV, NMR), NBO and first order hyperpolarizability analysis of N-phenylbenzenesulfonamide by density functional theory. *Spectroc. Acta Pt. A* **133**, 417–431 (2014). https://doi.org/10.1016/j.saa.2014.06.040.

[39] Tanış, E. Theoretical and experimental investigation of structural and vibrational spectra of 2-Methyl-1h-benzimidazole-5-carboxylic acid molecule. *Sakarya University Journal of Science* **21**, 545–563 (2017). https://doi.org/10.16984/saufenbilder.270275.

[40] Hughbanks, T. & Hoffmann, R. Chains of trans-edge-sharing molybdenum octahedra: metal-metal bonding in extended systems. *J. Am. Chem. Soc.* **105**, 3528–3537 (1983). https://doi.org/10.1021/ja00349a027.

[41] Małecki, J. G. Synthesis, crystal, molecular and electronic structures of thiocyanate ruthenium complexes with pyridine and its derivatives as ligands. *Polyhedron* **29**, 1973–1979 (2010). https://doi.org/10.1016/j.poly.2010.03.015.

[42] Chen, M., Waghmare, U. V., Friend, C. M. & Kaxiras, E. A density functional study of clean and hydrogen-covered α-MoO3(010): Electronic structure and surface relaxation. *J. Chem. Phys.* **109** 6854–6861 (1998). https://doi.org/10.1063/1.477252.